Kaien Zhang[1], Lizhen Huang[1], Jialin Mo[1], Bin Huang[1], Cheng Luo[1], Dezhong Yao[1], Pedro Antonio Valdes-Sosa[1], and Peng Ren[1]

[1]Affiliation not available

February 27, 2026

Abstract

The analysis of interactions among the human body's multiple physiological systems using information technology has recently emerged as a key focus in research. However, previous studies have typically treated each physiological system as a homogeneous entity, overlooking the fact that diverse physiological activities coexist even within individual systems. To overcome this limitation, the present study introduces a "physiological attribute network" framework. Using emotional stimuli-which elicit a wide range of physiological responses-as a case example, this framework extracts distinct attributes from each physiological signal to capture the heterogeneous physiological activities within individual systems, and enables network modeling at the level of physiological attributes. Key findings from this study demonstrate that individual physiological activities exert distinct and multifaceted influences both within and across physiological systems. Moreover, the study reveals dynamic synergistic and inhibitory interactions among these activities, highlighting their complex interdependencies. Importantly, it also demonstrates the adaptability of network topologies, which reconfigure in response to shifts in physiological states, such as emotional fluctuations. In summary, this work provides a fine-grained analytical framework for investigating physiological activities at both intra-and intersystem levels, offering significant potential to advance research in the fields of physiology and engineering.

Physiological Attribute Network: A Case Study of Emotion

Kaien Zhang, Lizhen Huang, Jialin Mo, Bin Huang, Cheng Luo, Dezhong Yao*, Pedro Antonio Valdes-Sosa*, Peng Ren* *Staff, IEEE,*

***Abstract*—The analysis of interactions among the human body's multiple physiological systems using information technology has recently emerged as a key focus in research. However, previous studies have typically treated each physiological system as a homogeneous entity, overlooking the fact that diverse physiological activities coexist even within individual systems. To overcome this limitation, the present study introduces a "physiological attribute network" framework. Using emotional stimuli—which elicit a wide range of physiological responses—as a case example, this framework extracts distinct attributes from each physiological signal to capture the heterogeneous physiological activities within individual systems, and enables network modeling at the level of physiological attributes. Key findings from this study demonstrate that individual physiological activities exert distinct and multifaceted influences both within and across physiological systems. Moreover, the study reveals dynamic synergistic and inhibitory interactions among these activities, highlighting their complex interdependencies. Importantly, it also demonstrates the adaptability of network topologies, which reconfigure in response to shifts in physiological states, such as emotional fluctuations. In summary, this work provides a fine-grained analytical framework for investigating physiological activities at both intra- and inter-system levels, offering significant potential to advance research in the fields of physiology and engineering.**

***Index Terms*—Emotion, physiological attribute network, network topology, inter- and intra- systems, non-Euclidean interaction.**

I. Introduction

THE human body is an extremely sophisticated and highly developed biological system. These systems are interdependent and dynamically interact, functioning as an organic whole to play a crucial role in maintaining homeostatic operations and ensuring the smooth functioning of vital processes. Information science has increasingly emphasized elucidation of cross-system interactions using physiological signals [1], [2]. Researchers have treated physiological signals including electroencephalography (EEG), electrocardiography (ECG), and electromyography (EMG) as distinct entities to analyze their mutual connections [3]. This emerging trend has led to the "physiological network" research paradigm, which conceptualizes signals as interconnected nodes [2]. Within this framework, network models are constructed by examining patterns of association between nodes to offer a comprehensive perspective on the dynamic interactions between multiple systems [4], [5]. Previous studies on applications across sleep, movement, emotion, and other fields have demonstrated the importance of investigating interactions between different physiological systems under various states [6]–[10].

However, this paradigm is not without its limitations. It tends to neglect the significant diversity of activities that occur within a single system. For example, when ECG signals are used as nodes in conventional network analyses, the detailed waveform components corresponding to specific cardiac events (e.g., P wave) remain indistinguishable at the network level. Moreover, conventional methods fail to capture opposing physiological functions encoded in ECG signals: low-frequency bands reflect sympathetic nervous system activity, while high-frequency bands correspond to parasympathetic regulation. To address these methodological shortcomings, this study introduces the "Physiological Attribute Networks" (PANs) framework. Unlike traditional approaches, this paradigm adopts a fine-grained perspective by extracting heterogeneous physiological attribute features from each physiological signal, thereby uncovering diverse activities within the same system. By analyzing the relationships among these attributes, it builds a comprehensive network which reveals both internal interactions among multiple activities inter- and intra- system interactions. By shifting the research focus from macroscopic system-level analysis to fine-grained investigation of diverse activities, this attribute-centric approach provides a more nuanced and biologically plausible model of human physiology.

It is widely recognized, distinct human emotions elicit corresponding response sequences from various physiological systems [9], [11], [12]. In existing literature, the research paradigm for emotion studies has shifted from in-depth analysis of single physiological signals to comprehensive exploration of multimodal physiological systems, with researchers seeking to extract diverse features from different physiological signals to precisely elucidate the intrinsic variation mechanisms of physiological states. For instance, Beatton et al. [13] analyzed heart rate variability-related (HRV-

This work was supported in part by National Key R&D Program of China under Grants 2024YFE0215100, in part by the National Natural Science Foundation of China under Grants 62171109, 82121003, 81871446, in part by Sichuan Provincial Science and Technology Project under Grants 2024JDHJ0064, in part by Chengdu Science and Technology Bureau Program under Grant 2022-GH02-00042-HZ and in part by the Major Scientific Research Project of the Ministry of Science and Technology under Grant STI 2030–Major Projects 2022ZD0208500.(First corresponding author: Peng Ren; Co-corresponding authors: Pedro Antonio Valdes-Sosa; Dezhong Yao.)

Kaien Zhang, Lizhen Huang, Jialin Mo, Bin Huang, Cheng Luo, Dezhong Yao, Pedro Antonio Valdes-Sosa and Peng Ren are with the Clinical Hospital of Chengdu Brain Science Institute, China-Cuba Belt and Road Joint Laboratory on Neurotechnology and Brain-Apparatus Communication, MOE Key Laboratory for Neuroinformation, School of Life Science and Technology, University of Electronic Science and Technology of China, Chengdu 611731, China.(e-mail: pren28@uestc.edu.cn, Pedro@uestc.edu.cn, dyao@uestc.edu.cn)

related) features and identified critical correlations, such as the negative relationship between certain frequency ratios and positive emotions, offering new perspectives on the autonomic nervous system's regulation. This research finding provides a novel perspective for understanding the relationship between emotions and the autonomic nervous system. Duan et al. [14] focused on EEG signals and found that differential entropy and its combinations significantly outperformed traditional energy spectrum features in emotion classification, with the gamma band showing a particularly strong correlation with emotional states. This discovery provides critical evidence for emotion classification research based on EEG signals. Brown et al. [15] investigated the synergy between multiple physiological indicators and subjective experiences, revealing that the consistency among these indicators varies significantly under different emotional intensities. This achievement facilitates an in-depth understanding of the physiological manifestation characteristics of emotions at different intensity levels. Wang et al. [16] combined multidimensional features from EEG and HRV, demonstrating that fusing multimodal features significantly improves classification accuracy and robustness compared to the limited information provided by unimodal signals. This research provides strong empirical support for the application of multimodal physiological feature fusion in emotion studies. However, existing multimodal physiological feature processing approaches mainly fall into two categories: screening emotion recognition-optimal features for targeted investigation, and concatenating all feature vectors as a multimodal fusion step prior to downstream recognition tasks. Yet these methods neglect the inherent non-Euclidean constraint relationships among physiological features, hindering the thorough revelation of complex interconnections between physiological activities. This study has proposed PAN framework enables in-depth exploration of physiological activity interactions, opening new avenues for emotion research and addressing the aforementioned gaps.

This study has investigated the nodes, edges, and global topology of PANs under different emotional states, and obtained the following findings.

(1). Physiological activities assume roles of varying significance in the functioning of physiological mechanisms across different emotional states. Notably, even within the same physiological system, these activities exhibit marked differences in their contributions. Furthermore, there is dual variability in their functional manifestations; even for the same physiological activity, distinct roles emerge both within its own system and when it interacts with other systems. Additionally, these roles are not static but can dynamically change depending on an individual's emotional state.

(2). For the first time, this study clearly demonstrates two distinct types of interrelationships among physiological activities, whether within a single system or across multiple systems: synergistic and inhibitory effects. Even for the same pair of activities, their synergistic and inhibitory effects are not static, but rather exhibit dynamic changes. These effects may even transition from synergistic to inhibitory or vice versa, based on an individual's emotion state.

(3). It observes differences in the overall topological structures of attribute networks across emotion states, indicating that the collective behavior of all physiological activities undergoes dynamic adjustment in response to changes in these emotion states.

The construction of the four PANs for emotions, as well as the changes in topology (including nodes, edges, and global properties) across different emotional states, will be elaborated in detail later in this paper.

II. Method and Materials

A. Physiological Attribute Extraction

The DEAP dataset [17], [18] comprises multimodal physiological signals collected from 32 physically and mentally healthy participants, evenly divided between males and females. During the experiment, each of the 32 subjects was required to view 40 videos, each lasting one minute, while their physiological signals were recorded. It is important to emphasize that the effectiveness of these videos in evoking emotions was evaluated during the pre-evaluation phase of the public experiment.

The physiological signals recorded in the DEAP dataset include EEG signals collected by 32 electrodes placed in accordance with the international 10-20 electrode placement system, as well as a series of signals reflecting the activities of other physiological systems: photoplethysmography (PPG), trapezius electromyography (tEMG), zygomatic electromyography (zEMG), temperature (TMP), respiration (RSP), and galvanic skin response (GSR). Based on the pre-recorded emotional experiment ratings in the DEAP dataset, the above signal data were divided into four categories in this study, namely high arousal-high valence (HAHV), high arousal-low valence (HALV), low arousal-high valence (LAHV), and low arousal-low valence (LALV). Then, four most representative groups of signals corresponding to each emotion were selected from the four emotional categories, which were combined as the overall sample of this study (see Fig.1, left part). Existing studies based on the DEAP dataset have confirmed that 12 specific EEG channels (T7, CP1, Oz, F8, FC6, FC2, Cz, C4, T8, CP6, CP2, and PO4) have the strongest correlation with the emotional processing of individuals. Meanwhile, relevant studies [19], [20] have shown that the HRV index can be effectively characterized by virtue of the variability characteristics exhibited in PPG signals. Therefore, this study followed the conclusions of previous studies to extract signals from the above 12 EEG channels and adopted PPG signals as indicators for characterizing the activity of the HRV system. Then comprehensive attribute extraction was performed on these signals and the signals of the remaining peripheral physiological systems, and the ReliefF algorithm was applied for attribute selection (see Fig.1, middle part). Finally, the top 48 weighted multi-system attributes were selected. After obtaining various physiological activity attributes of the multimodal physiological systems, the Extended Bayesian Information Criterion for graphic lasso (EBICglasso) method was used in this study to construct four groups of PANs (see Fig.1 right part, Fig.2a), and a comparative analysis of these PANs was conducted at the global, edge and node levels (see

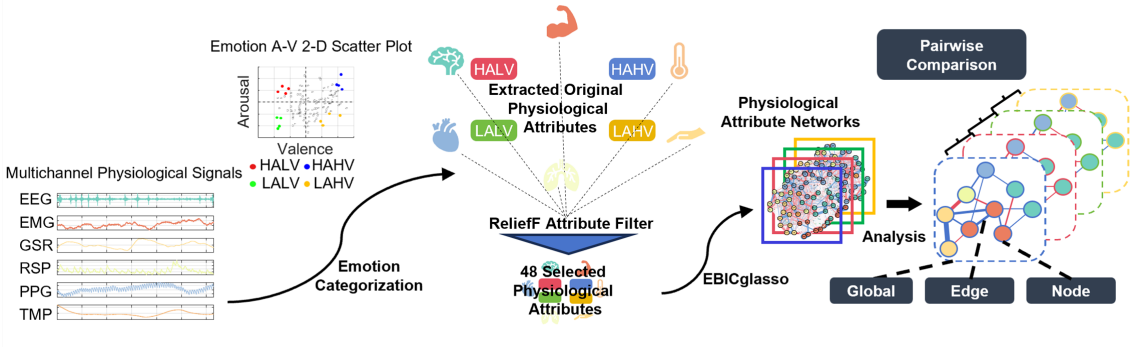

Fig. 1. Experimental workflow and analysis pipeline.

Fig.1, right part), yielding promising results. Table 1 in the Appendix elaborates on the specific information of these 48 attributes, and Table 2 briefly summarizes the physiological significance of each attribute in emotional regulation.

B. Network Construction

The EBICglasso operator [21] is an advanced technique for estimating sparse networks on high-dimensional data, which combines the glasso method for estimating sparse data and the EBIC for model selection [22], [23]. This technique enables the precise selection of optimal regularization parameters to construct sparse, stable attribute networks. Technically, EBICglasso is well-suited for the high-dimensional physiological data in our research, which typically involve numerous variables with complex collinearity. The glasso algorithm addresses this issue via regularization-based maximum likelihood estimation, with its core objective function expressed as follows:

$$\hat{\Omega} = arg\min_{\Omega>0}\{tr(S\Omega) - logdet(\Omega) + \lambda \left\|\Omega\right\|_1\} \quad (1)$$

In the above formula, $S = \frac{1}{n}X^T X$ is the sample covariance matrix. Ω is the precision matrix of X, which $X = [x_1, x_2, \ldots, x_n]^T$ is vector of observed data. $tr(S\Omega)$ is the trace of the matrix $S\Omega$. λ is a regularization parameter that controls the sparsity of the model. $\left\|\Omega\right\|_1$ is the L1 norm of Ω, the sum of the absolute values of all elements. L1 regularization forces weak or redundant elements in Ω to zero, retaining only statistically significant non-zero elements—these correspond to edges between physiological attributes in the network, reflecting conditional dependencies (associations remaining after controlling for other attributes). This sparsification reduces complexity and avoids obscuring core patterns with noise associations, clarifying key physiological interactions. The EBIC selects the optimal λ [24]. It adds a penalty for model complexity to the traditional BIC, balancing fit and generalization for high-dimensional data:

$$EBIC(\lambda) = -2logL(\hat{\Omega}) + log(n)\cdot df(\lambda) + 4\gamma log(p) \quad (2)$$

$logL(\hat{\Omega})$ is the log-likelihood function. n is the number of samples. $df(\lambda)$ is the degree of freedom of the model, i.e. the number of non-zero elements. p is the number of variables. n is the sample size. γ is an adjustment parameter, usually taking a value of 0.5 or 1. When $\gamma = 0$, EBIC degenerates into BIC. For physiological data with limited samples and individual variability, EBIC dynamically adjusts penalties to avoid overfitting to noise or oversimplification, ensuring network stability across samples. This study sets the $\gamma = 1$ for reducing false positive edges in the network and ensures the network is accurate and reliable.

EBICglasso selects λ and constructs networks via grid search and preliminary estimation: Compute precision matrices for predefined λ values using glasso, generating candidate network structures to accommodate diverse potential associations between physiological attributes. For each candidate matrix, compute EBIC using $df(\lambda)$ and likelihood values. The λ minimizing EBIC is selected data-dependently, avoiding subjective bias. The network is built from the precision matrix γ estimated with optimal λ, where non-zero elements represent conditional dependencies. Four PANs constructed by this process addresses high-dimensionality and sparsity, supporting the subsequent edge accuracy and centrality robustness testing in this study.

C. Network Comparison Test Analysis Method

The Network Comparison Test (NCT) is a statistical method used to compare significant differences in global network structures between different emotional states [25]. The main steps of NCT are as follows:

(1). Networks are built based on metrics such as correlation or co-occurrence frequency. In this paper, networks are constructed using correlation and the EBICglasso graphical operator.

(2). Weights are assigned to each edge in the network. For the weight analysis of PANs, this paper adopts the non-parametric Spearman correlation coefficient which is suitable for non-linear, non-normally distributed data, and can effectively capture monotonic associations between physiological attributes, which is more consistent with the complex characteristics of physiological signals.

(3). Permutation tests or other statistical methods are used to compare differences in edge weight distributions between two groups of networks. In this paper, 500 sampling permutation tests are performed using the bootstrapping to compare differences in weight distributions between networks. The algorithm

performs normalization on the input network data of each group to ensure that edge weight comparisons are based on a unified magnitude benchmark.

As the core statistical method for inferring the significance of differences in NCT, bootstrapping permutation test works by randomly rearranging data to construct a null hypothesis distribution [26], [27]. This method does not rely on the distribution of data and is particularly applicable to data such as network edge weights that may not conform to the normal distribution.

D. Edge Analysis

The number of synergistic edges and inhibitory edges in each emotional PAN was calculated in this study, while the connections between nodes intra-system and those inter-systems were statistically analyzed. Specifically, synergistic edges and inhibitory edges were used to decompose the functional attributes of edges. The number, density and dynamic changes of synergistic and inhibitory edges in intra-system/inter-system contexts were statistically examined to analyze differences in physiological interactions under emotional stimuli.

In the edge analysis, pairwise comparisons of each emotional network were conducted via NCT, and the network connection edges with significant differences between various emotions were identified to analyze the interaction differences among physiological attributes under different emotional states. Like the global NCT comparison, Spearman's correlation coefficient was adopted to assign weights to individual edge differences. This approach is well-suited to the nonlinear and non-normal characteristics of physiological signals, enabling the capture of associations between edges. A total of 500 permutation tests were performed using the bootstrapping to construct a null hypothesis distribution. The position of the observed edge weight difference relative to the null distribution was then compared to calculating the p value. To ensure the stability and non-randomness of edge connections, 500 rounds of bootstrapping with replacement were employed to verify the downsampled means of edge weights and their 95% confidence intervals, thus guaranteeing the robustness of the network edges.

E. Node Analysis

In this study, centrality analysis was adopted to explore the roles of physiological attribute nodes in the network. Global centrality reflects the role of physiological activities in the interaction of overall attributes, while bridge centrality characterizes the role of activities in the interaction across cross-physiological systems [28].

Strength: This metric quantifies the activity of attribute nodes from the perspectives of information transmission and resource interaction. A higher strength value of a node indicates that the activity represented by this node plays a more important role in network connectivity. Specifically, the Global Strength (G-Strength) reflects the activity level of the target activity in the interactions within the entire PAN, while the Bridge Strength (B-Strength) only represents the interaction capacity of this activity with other activities across cross-systems. The formula for Strength centrality is given by:

$$G\text{-}Strength_i = \sum |k_i| \tag{3}$$

$$B\text{-}Strength_i = \frac{\sum |k_{io}|}{\sum |k_{in}|} \tag{4}$$

In the formula, i denotes a specific activity node. $|k_i|$ represents the absolute value of the weight of edges directly connected to node i in the calculation of G-Strength. In the calculation of B-Strength, $|k_{io}|$ denotes the absolute weight of the connecting edge between different systems relative to the target node i and $|k_{in}|$ denotes the absolute weight of the connecting edge within the same system as the target node i.

Betweenness: This metric reflects the capacity of an activity to control the information flow within the PAN, thereby characterizing the efficiency of information transmission associated with the target activity. The Global Betweenness (G-Betweenness) centrality reflects the information flow control capacity of a node in the entire PAN, while the Bridge Betweenness (B-Betweenness) centrality only represents the information flow control capacity of a node across different systems. The formula for Betweenness centrality after normalization (to make the result < 1) is:

$$G\text{-}Betweenness_i = \frac{1}{(N-1)(N-2)/2} \sum_{s \neq i \neq t} \frac{n^i_{st}}{g_{st}} \tag{5}$$

$$B\text{-}Betweenness_i = \frac{1}{(N-1)(N-2)/2} \sum_{s_o \neq i \neq t_o} \frac{\hat{n}^i_{s_o t_o}}{\hat{g}_{s_o t_o}} \tag{6}$$

For G-Betweenness, n^i_{st} represents the number of shortest paths passing through the physiological activity node i and connecting another two activity node s and t, g_{st} denotes the total number of shortest paths connecting activities s and t. And for B-Betweenness, $\hat{n}^i_{s_o t_o}$ represents the number of shortest paths that begin from and end to two nodes in the systems different from node i and pass through node i. $\hat{g}_{s_o t_o}$ refers to the total number of shortest paths passing through the activity node i and connecting another two activity nodes s_o and t_o that belong to different systems from node i.

ExpectedInfluence: This metric quantifies the synergistic and inhibitory relationships among activities, with simultaneous consideration of both positive and negative impacts induced by node connections. The value close to zero indicates that the target activity exerts a relatively balanced influence; a positive value means the activity has a significant synergistic effect, while a negative value implies that its dominant effect is inhibitory. Similarly, the Global ExpectedInfluence (G-ExpectedInfluence) reflects the synergistic and inhibitory capacity of an activity in the entire network, and the Bridge ExpectedInfluence (B-ExpectedInfluence) only characterizes the synergistic and inhibitory capacity of a node across different systems [23]. The formula for ExpectedInfluence is:

$$G\text{-}ExpectedInfluence_i = \sum k_i \tag{7}$$

$$B\text{-}ExpectedInfluence_i = \frac{\sum k_{io}}{|\sum k_{in}|} \tag{8}$$

Consistent with Strength centrality, k_i represents the weight of the edge directly connected to node *i*. In bridge centrality analysis, k_{io} denotes the weight of the connecting edge between different systems relative to the target node *i* and k_{in} denotes the weight of the connecting edge within the same system as the target node *i*.

III. Result

A. Network Comparison Test by Emotional States

The results of NCT indicated that all pairwise comparisons, with the exception of direct comparison between HALV and LAHV, exhibited highly significant differences in overall network connectivity (p value < 0.01). This finding underscores the substantial impact of emotional state on topological configuration of physiological activity, suggesting that different emotions elicit distinct patterns of physiological integration.

Notably, while no significant differences were observed in global network topology between HALV and LAHV, marked variation emerged for specific connections. For instance, interaction between EEG nodes E9 (sample entropy) and E5 (spectral power) demonstrated significant discrepancies, as did connectivity patterns among peripheral physiological system nodes, such as the D5 node of HRV system and the G8 node of GSR system.

To ensure the reliability of these findings, robustness validation was conducted for both the network edges and nodes [29]. Bootstrap sampling was employed to evaluate the correlation between the original sample and the results obtained from data with missing values. Even with 50% of data missing, the correlation between the centrality of the sampled points and the original sample remained above 0.5 (Fig. 2(b)). This finding satisfies the criteria for strong robustness [30], which defines the correlation threshold as ≥ 0.5 and sets a minimum allowable threshold of no less than 0.25; a value below this minimum threshold may suggest potential randomness in network construction [31]. For edge robustness validation (Fig. 2(c)), this study calculated the bootstrap mean and confidence interval (CI) of edge weights through sampling. These computed values were then compared with those of the original weights (the sample). The results demonstrated that correlation errors consistently remained within an ideal range, thereby comprehensively validating both stability and non-randomness in the network construction.

B. Network Edge Analysis Based on Different Emotional State

The primary focus of this study was to research the network connectivity among each "physiological aggregated system" – each of which also encompasses a range of physiological activities (Fig. 3). Notably, the intra-system activity connection density fluctuates consistently within the range of 0.70-0.74, while edge density for inter-system connections ranges from 0.42-0.43 (Fig. 3(a)). Particularly noteworthy is the LALV network, where the connection density drops to 0.37 – lower than the density ratios observed in other emotional networks. These findings indicate relatively low overall inter-system connection densities. These inter-system edge densities also exhibit considerably more variability across emotional states than those intra-systems.

(1). Based on the data shown in the diagonal elements (Fig. 3(b)), the edge density reaches its peak within the circulatory system in HAHV. Conversely, in LAHV, the nervous system becomes the most interconnected, exhibiting the highest edge density. Notably, in this state, TMP activity is isolated from other systems, indicating relative autonomy of the temperature regulation mechanism. Additionally, in HALV, the edge density attains its maximum within the motor system. Furthermore, internal connections demonstrate relatively minor variation within both the GSR system and RSP system across all four emotional states, suggesting a certain degree of stability. Meanwhile, their edge densities are higher than those observed within either the circulatory or nervous systems with these stable patterns. (2). The off-diagonal elements lead to several key findings (Fig. 3(b)). First, emotional state exerts a stronger influence on inter-system than on intra-system connections. To elucidate this finding, this study further examined the relationship between the HRV system and RSP system. The connections between these systems demonstrate considerable variability across emotional states: in LALV, the edge density between HRV and RSP was measured at only 0.34, markedly lower than the 0.45-0.50 recorded in the other three states. Similarly, pronounced differences were observed in edge density between the EEG system and GSR across all four emotional states. Specifically, in LAHV, this edge density peaked at 0.59, while remaining relatively stable within the range of 0.45-0.52 in the other three states. Furthermore, distinct variations in inter-system connectivity were observed under high valence versus low valence conditions. Notably, under high valence, the edge densities between HRV and TMP ranged from 0.63-0.67 – apparently higher those under low valence conditions.

We also investigated the synergetic and inhibitory subnetworks associated with various physiological activities (Fig. 3(c)). (1). intra-system synergetic subnetworks exhibited a greater degree of development under different emotional states than their inhibitory counterparts. Conversely, the progression of synergetic and inhibitory subnetworks within inter-system contexts was found to be nearly equivalent. In the synergistic subnetwork, apparent variation was observed across emotional states. For instance, the number of synergistic connections in the E7 node fluctuates markedly with changes in emotional state. Specifically, it exhibits the fewest intra-system synergistic connections in LALV, and the most in HAHV. Furthermore, the R6 node within the RSP system also demonstrates considerable fluctuations in inter-system synergistic effects, achieving its maximum level of synergistic connections in HALV. Additionally, distinct emotional states sometimes induce strong alterations in inhibitory subnetworks. For example, in HALV, the G5 node exhibits five inhibitory connections, whereas it possesses only one connection in LALV. Furthermore, the G7 node within the GSR system demonstrates twelve inhibitory connections in HALV, but only three in LALV and LAHV. (2). The relationships between synergistic and inhibitory subnetworks demonstrated both specificity and variability across emotional states. For instance, the

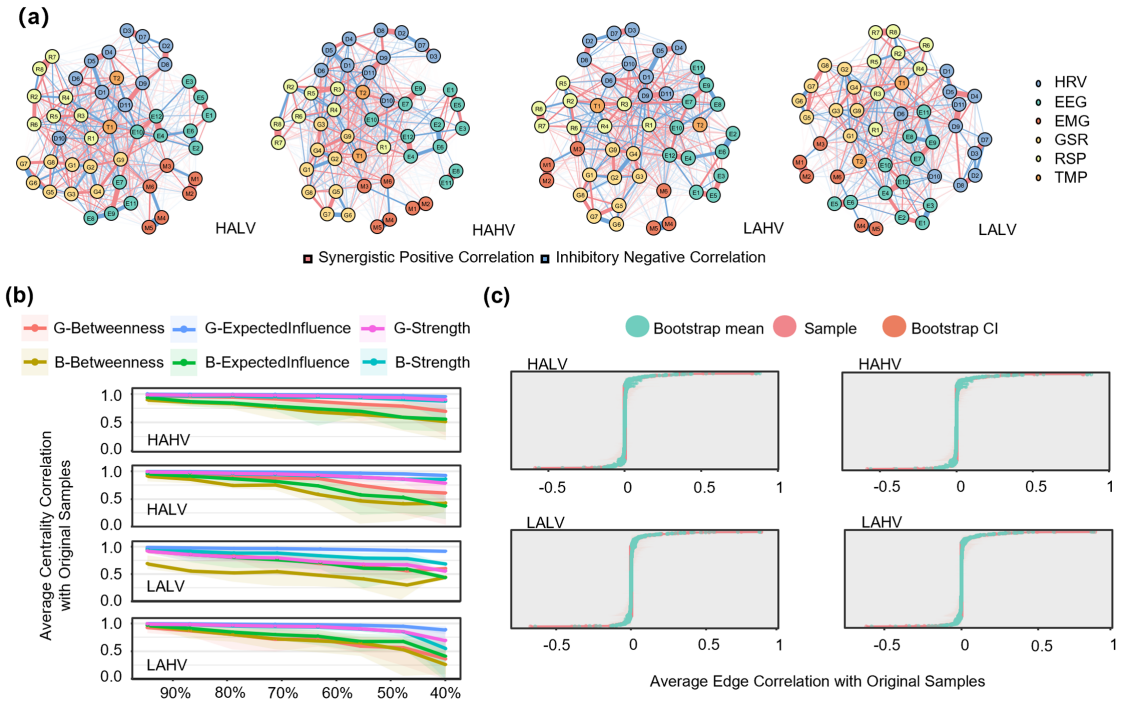

Fig. 2. (a). Network visualization for the four emotional quadrants. Nodes represent physiological attributes from the six systems (color-coded); red edges indicate synergistic correlations, while blue edges indicate inhibitory correlations. (b). Robustness of node global centrality and bridge centrality. The x-axis represents the percentage of resampled data relative to the total original data; the y-axis represents the correlation between the resampled centrality metrics and original centrality metrics. The correlation between the resampled centrality metrics and original metrics remained above 0.5 even with less than 50% of the total original data, meeting the criterion for strong robustness ($\geq$ 0.5). (c). Robustness of edge connectivity. The x-axis represents all correlative edge weights in the network (ranging from -1 to 1), while the y-axis represents the edges present in the network (omitted in the figure). The average edge weights derived from bootstrap downsampling (blue) showed substantial overlap with those from the original data (red); furthermore, the 95% confidence interval (CI, orange shading) of the downsampled data was narrow, confirming highly stable edge weights and non-random network construction.

M1 node exhibits remarkably stable intra-system synergistic or inhibitory activities across emotional conditions, in stark contrast to other nodes, which display dynamic changes in their connection patterns. Furthermore, D6 exhibits its maximum synergistic connections in HAHV, while its inhibitory connections increase in LALV. The fluctuations observed in inhibitory connections for the E11 node are primarily driven by the valence dimension, whereas those for the G7 node are predominantly influenced by arousal.

Pairwise comparisons were conducted on the edges of four distinct emotional networks (Fig. 4). Among all network comparisons, the most significant differences in edge counts were found between the LALV and HALV networks, while the HAHV and LAHV networks exhibited minimal differences. (1). Across all network comparisons, disparities in edge counts predominantly arose from intra-system rather than inter-system connections. For instance, 22 edges exhibit intra-system differences between the LALV and HALV networks, compared to only 13 edges showing inter-system differences. Even within the HAHV and LAHV comparison – which displays the least overall difference – 12 edges within each system still reveal disparities. (2). The nervous system exhibited the largest differences in edge count across all systems in pairwise comparisons between emotional networks. Furthermore, substantial diversity was observed within these comparisons. For example, when contrasting LALV with LAHV, as well as LALV with HALV, the primary distinctions are evident in the connections among the nodes which represent the spectrum distributions of EEG signals (e.g., E1-E6). In contrast, differences primarily arise in the nodes describing the entropy of EEG signals during comparisons between HALV and HAHV, as well as between HAHV and LAHV. (3). Specific connections also demonstrated characteristics unique to specific emotions. For instance, the M4-M6 and D1-G5 edges demonstrate differences exclusively in the network comparisons between HAHV and LALV. Similarly, the D1-E2 and R2-R3 connections reveal differences only when comparing HALV and LAHV. Furthermore, the G9-R8 edge shows variation solely in the comparison between HAHV and HALV.

C. Network Node Analysis Based on Different Emotional States

Two primary methods were employed to characterize the node's properties. First, a global centrality metric was utilized to assess their roles across the entire network (encompassing all systems), intuitively indicating their core status within the overall network structure [32]. Second, a bridge centrality metric was introduced, reflecting the interaction of one node with those in other physiological systems. This approach underscores the critical role these nodes play in facilitating cross-system connections [33]. Building upon the previously discussed centrality metrics, this study further introduced

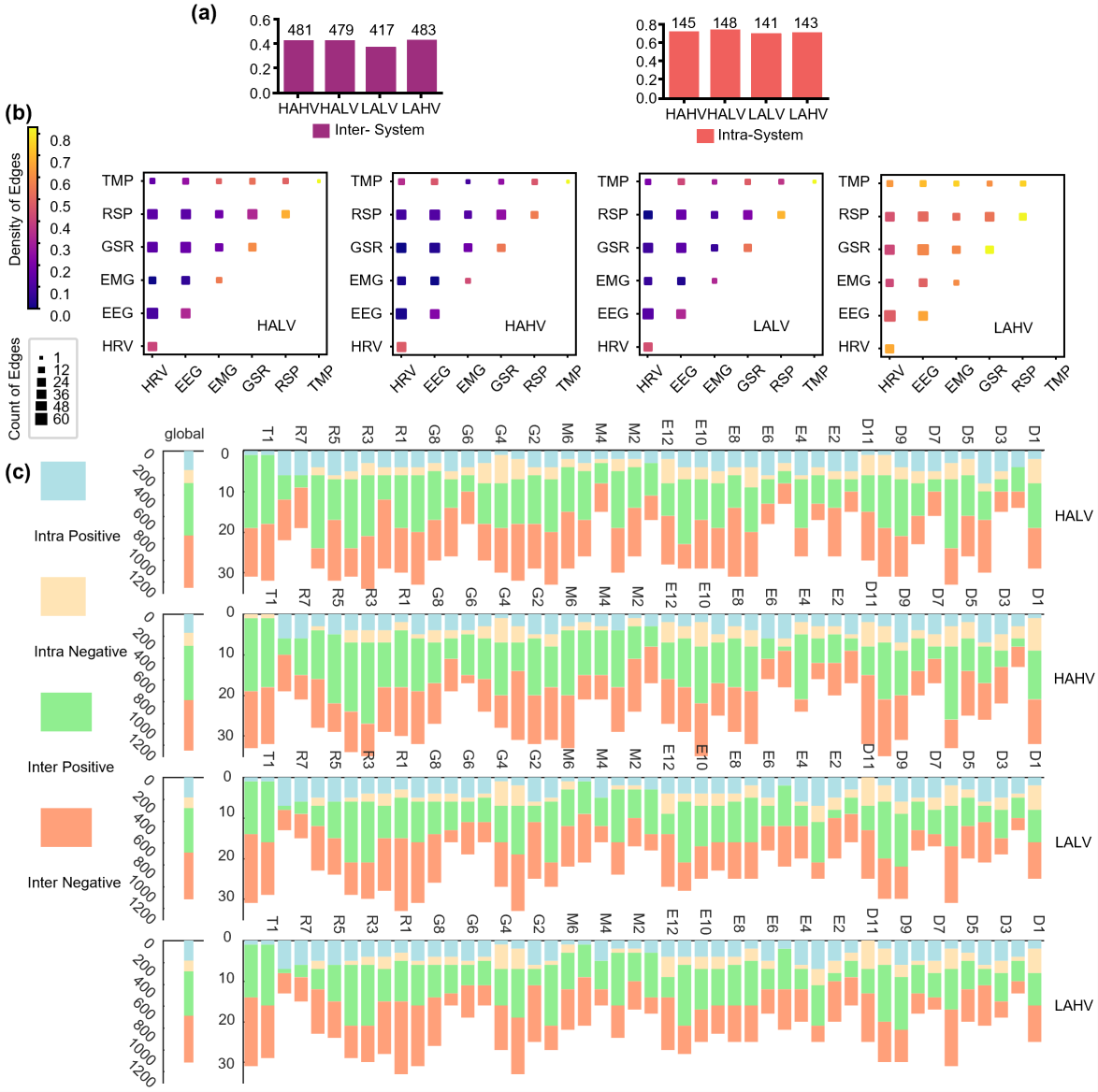

Fig. 3. (a). The bar charts display the total connection density (represented by the y-axis) and the total number of edges (indicated by the numbers above the bars) within all physiological systems (left bars) and between all physiological systems (right bars) under the four emotional states. (b). In the heatmap, the color intensity represents the magnitude of connection density, and the square size represents the magnitude of the number of edges. (c). Each bar is color-coded to represent different connection types of individual nodes under each emotion: blue for intra-system synergistic connections, yellow for intra-system inhibitory connections, green for inter-system synergistic connections, and orange for inter-system inhibitory connections. The x-axis indicates the cumulative number of edges. Due to space limitations, the names of some intermediate nodes are omitted along the y-axis. The "global" section at the bottom further calculates the total number of each connection type across all nodes in each emotional network.

refined measures to quantify node functions with enhanced precision.

Through a more detailed examination of centrality for each individual system, the following patterns can be discerned (Fig.5(a),(b)). (1). In each of the emotional states, physiological activities linked to the nervous and motor systems exhibit apparently lower B-Strength in comparison to other systems. This may imply that these activities primarily fulfill crucial roles within their native systems. Conversely, physiological activities associated with TMP and the RSP system display higher B-Strength, suggesting that these activities facilitate cross-system information exchange. (2). The G-Betweenness of each physiological system is generally higher than its corresponding B-Betweenness, which indicates that physiological activities within native systems tend to operate with greater efficiency relative to those involved in cross-system interaction. Additionally, apparent variation in B-Betweenness is observed between emotional states. For instance, under HAHV, the B-Betweenness of EEG, HRV, GSR, and TMP systems are lower than that under other emotional conditions. Similarly, in HALV and LAHV, GSR systems demonstrate the highest B-Betweenness. Under LALV, in contrast, both EEG and GSR exhibit the largest B-Betweenness. (3). Analysis of ExpectedInfluence underscores the complexity of phys-

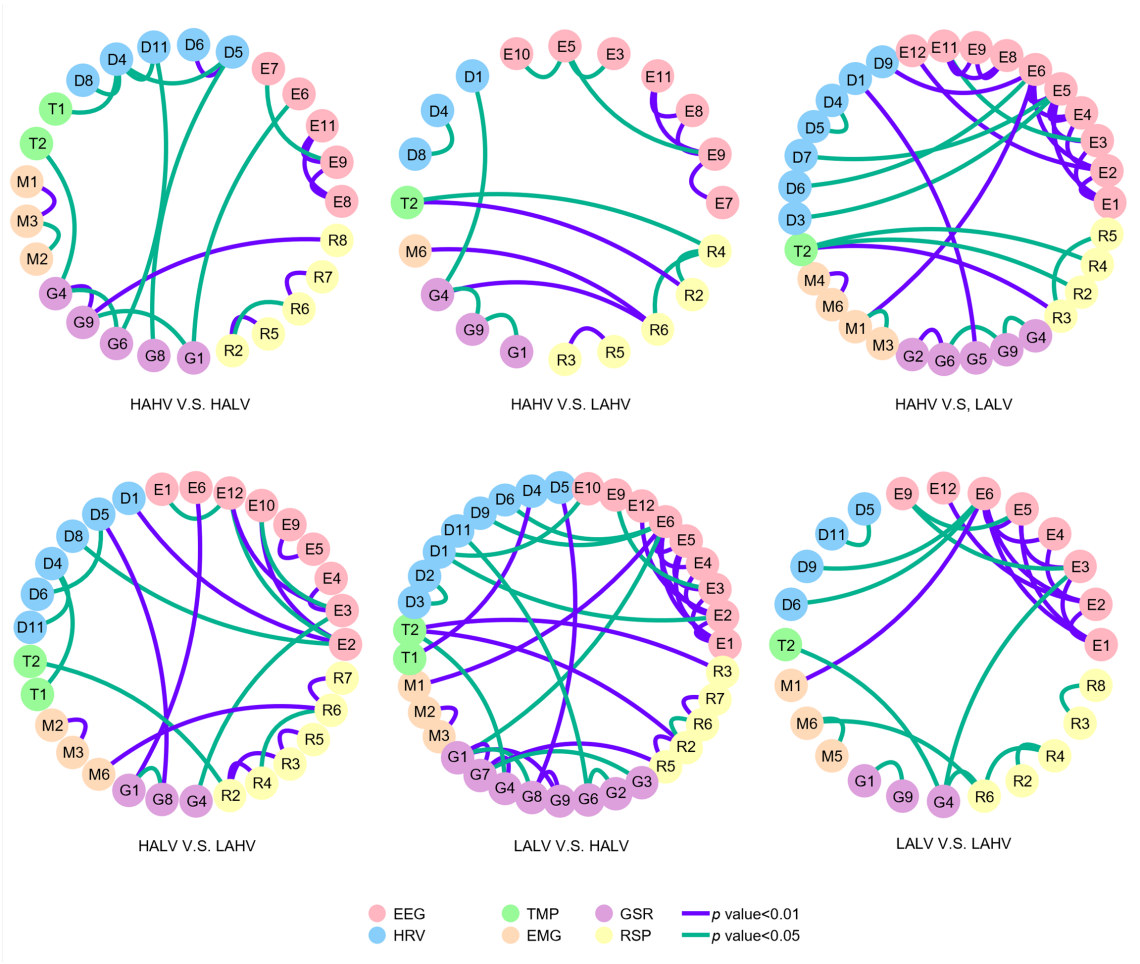

Fig. 4. The six subplots show all connections with significant edge weight differences under all pairwise comparisons of the four emotional networks. Physiological attribute nodes at both ends of the edges are color-coded to distinguish the systems they represent. The purple edges indicate connections whose differences are significant at the p value$<$0.01 level when comparing the two emotional networks, while green edges indicate significance at p value$<$0.05. In network comparisons, FDR correction is performed to guarantee the reliability of the results.

iological activities involved in emotional regulation. Under LALV, the nervous system predominantly displays synergistic effects, both within the overall network and across inter-system connections (B-ExpectedInfluence $>$ 0). In other emotional states, in contrast – particularly in LAHV, where B-ExpectedInfluence $<$ 0, inter-system connections tend to show more inhibitory effects. Nevertheless, nodes within the nervous system continue to primarily demonstrate synergistic effects within the overall network (ExpectedInfluence $>$ 0.3).

After analyzing centrality of individual systems level, the research subsequently explored the physiological activity levels represented by the nodes (Fig. 5(c),(d)). (1). Strength presents a wide range of diverse patterns that can be systematically categorized and analyzed. Certain nodes, such as D9, exhibit dominance within their internal system structure, but weak external importance. Some, like E5 and E6, display distinct differences in their two types of Strength response patterns, with their B-Strength surging to over 10 under in LALV, apparently higher than in other emotional states; nevertheless, their G-Strength is the smallest here among all emotional states. The node behavior is variable, however, and other nodes demonstrate relatively stable G-Strength responses across emotional contexts. Certain nodes, exemplified by M3, show remarkable stability across emotions. (2). HRV nodes, including D2 and D7, maintain nearly constant G-Strength across emotional states, reflecting relative homeostasis within the cardiovascular system. Despite these general patterns, however, notable exceptions also exist. For instance, D1 exhibits considerable variability across the four emotional states (i.e., variance = 0.23), apparently higher than other HRV nodes. In LALV, it displays both the lowest G-Strength (i.e., value = 1.34) and peak B-Strength (i.e., value = 11.82). Furthermore, D9, D10, and D11 exhibit relatively low G-Strength, but considerable variation in B-Strength across emotional contexts. Finally, the centrality characteristics of nodes within the peripheral physiological system show variability. G4 demonstrates high B-Strength (i.e., average value = 11.29) with minimal variation, while G2 has an average B-Strength of 6.52, with values of 8.16 and 5.33 under LALV and LAHV, respectively. (3). The nodes exhibit diverse characteristics across different emotional states for the G-Betweenness and B-Betweenness metrics. Certain nodes, such as D3, D7, and M5, demonstrate a consistent lack of G-Betweenness and B-Betweenness functionality; additionally, D10 is notable for its absence of B-Betweenness. Furthermore,

both G-Betweenness and B-Betweenness reveal specificity contingent upon the emotional state. For instance, D2 and T2 possess B-Betweenness exclusively in HALV, while M2 only exhibits G-Betweenness functionality in LALV (But its G-Betweenness still remains very low). Finally, the nodes with the highest G-Betweenness and B-Betweenness values differ across various emotional states. In HAHV, for example, nodes M3, G9, and R4 are predominant, while HALV primarily relies on E10 and G4, LAHV is chiefly dependent on D9, and LALV is predominantly influenced by E5 and G4. (4). G-ExpectedInfluence and B-ExpectedInfluence reveal the distinct roles that nodes play within the overall network and across systems, particularly regarding effect polarity. Differentiation in node effect polarity is observed in the cardiovascular system: D1 exhibits an inhibitory effect within the overall network, with an average ExpectedInfluence of -0.79 across all four emotional states, yet also strong synergistic effects in cross-system connections, averaging 3.89 for B-ExpectedInfluence. In contrast, Nodes D2, D3, and D4, in contrast, display synergistic effects within the overall network, with respective mean ExpectedInfluence values of 1.15, 1.09, and 0.71, but strong cross-system inhibitory effects, averaging -3.91, -3.77, and -4.71 for B-ExpectedInfluence. Furthermore, certain nodes, such as D5 and D6, demonstrate reversals in their ExpectedInfluence polarity during emotional transitions; for instance, D5 inhibits network activity under HAHV and LAHV conditions, but shifts to a synergistic role in HALV and LALV. This dynamic behavior is not exclusive to the cardiovascular system. For example, E8 also displays inhibitory cross-system effects in HALV and LALV, but transitions to a synergistic role under HAHV and LAHV, as its B-ExpectedInfluence.

IV. Discussion

A. Total Differences between Networks

Initial network comparison tests were conducted to uncover the topological disparities in PAN across diverse emotional states. Specifically, in high-arousal contexts, a distinct pattern of highly efficient connectivity becomes evident, with inter-system connection densities ranging between 0.42 and 0.43. Notably, HRV system and RSP system demonstrate significant reinforcement in inter-system links, which is likely due to the heightened excitability of the sympathetic nervous system, which orchestrates synchronous activation of the heart rate and respiration. This synchronization consistent with arousal-dependent modulation of thalamo-cortical interaction [34]. Conversely, LALV is marked by modular isolation, including the lowest observed inter-system connection density of 0.37. The only fundamental synergistic interactions this state preserves are between TMP system and RSP system. This result may stem from the energy conservation response of the parasympathetic nervous system, which minimizes redundant connections.

Concurrently, EEG data reveal a high degree of internal physiological coordination within the brain, potentially contributing to the modular isolation observed in this emotional state. Interestingly, despite the absence of significant differences in global network topology between HALV and LAHV (p value > 0.05), pronounced discrepancies in edge connections emerge between physiological activities. These discrepancies involve EEG sample entropy, spectral energy nodes, and peripheral systems (e.g., D5 and G8), indicating that emotional transitions induce precise modifications in the correlations between physiological activities, which is consistent with the distinction between emotional states, concepts, and experiences [35]. Moreover, emotion-specific differential edges within each network provide further insight into this precise regulatory mechanism. For instance, the G9-R8 edge exhibits variation exclusively between HAHV with HALV, serving as a biomarker to differentiate positive from negative high-arousal emotions. Similarly, the D1-G5 edge displays significant differences only between HAHV and LALV, underscoring cooperative activation within the cardiovascular-sweat gland system during HAHV – a collaboration notably absents in LALV – thereby further substantiating the modular isolation attribute of LALV. These findings align with and extend observations made in previous studies, offering a more nuanced understanding of the influence of emotional state on the topological structure of PAN.

B. Synergetic and Inhibitory Networks

This study innovatively investigates synergetic and inhibitory networks across physiological activities. A significant finding is that within individual physiological systems, synergetic networks predominantly outnumber inhibitory one. This general tendency towards mutual cooperation likely arises from the relatively low heterogeneity among physiological activities within the same system. Such environments inherently promote synergetic interaction, as physiological activities within a single system typically share similar functional objectives and regulatory mechanisms. When the analysis extends to connections between systems, however, a more balanced distribution of synergetic and inhibitory links becomes apparent, reflecting the increased heterogeneity and complexity of interactions between systems, each characterized by its unique set of physiological functions and regulatory pathways. This heightened complexity necessitates a more nuanced interplay between synergy and inhibition to sustain overall homeostasis. A particular notable finding pertains to the enhancement of cross-system inhibitory connections in EEG signals during high-arousal states, as compared to low-arousal states. This phenomenon plays a crucial role in filtering out irrelevant physiological activities, thereby facilitating more focused and efficient engagement in emotional processing tasks [36], [37]. Such refinement of physiological responses is essential for adaptation to the increased demands associated with high-arousal situations. Within the nervous system itself, apparent variation in synergistic and inhibitory tendencies is observed between physiological activities. For instance, EEG sample entropy is primarily associated with cross-system inhibition, indicating its function in regulating and synchronizing activities across peripheral nervous systems.

Conversely, power spectrum analysis reveals a greater inclination towards cooperation within the same physiological system, particularly under LALV. In this context, positive

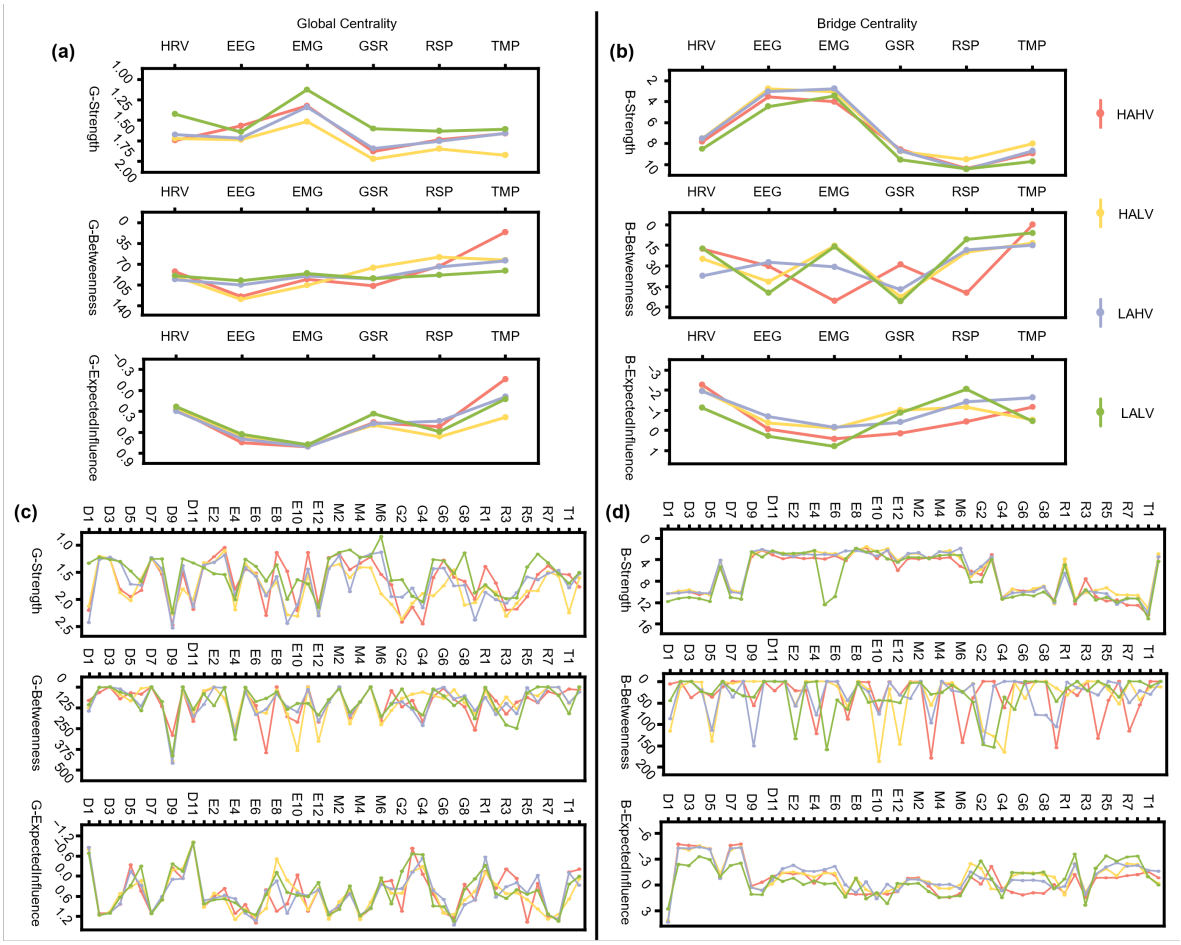

Fig. 5. The line chart uses different colors to denote different emotional states. For space efficiency, the names of intermediate nodes are omitted every three nodes along the y-axis. (a). Average global centrality of physiological activities represented by each physiological system. (b). Average bridge centrality of physiological activities represented by each physiological system. (c). Global centrality at the physiological activity level. (d). Bridge centrality at the physiological activity level.

intra-system correlations of spectral attributes establish a foundation for functional integration across brain regions, thereby promoting coherent cognitive and emotional responses [38]. In physiological systems such as HRV system, intra-system cooperation is essential for maintaining cardiovascular homeostasis, consistent with established norms and metrics of HRV [39]. Concurrently, cross-system inhibition, mediated by the parasympathetic nervous system, serves to mitigate excessive peripheral variation, thereby preventing physiological overload. This mechanism aligns with the principle proposed in psychological research of reducing physiological variation errors, and resonates with the free-energy principle [40], which emphasizes minimization of prediction errors in biological systems [41].

Our findings highlight the dual role of specific physiological activities—e.g., node D1 in the HRV system. Within its own system, D1 acts primarily as an inhibitory internal regulator for cardiovascular stability, yet collaborates across systems to facilitate cross-system communication and coordination. This versatility underscores that physiological activities may adopt distinct roles based on contextual factors and physiological state.

C. Centrality Analysis of Networks

Moreover, this study employs centrality analysis as a robust methodological framework to dissect and elucidate the distinct roles of physiological activities. Below is a more refined and logically structured explanation, incorporating insights from the provided documents [23], [28]. (1). We meticulously examine two sub-indices of Strength(i.e., B-Strength and G-Strength), revealing pronounced functional differentiation between physiological activities. Specifically, those tied to TMP and RSP rate exhibit markedly higher B-Strength, suggesting their pivotal role as conduits for seamless interaction across diverse systems [42]. In contrast, EEG and EMG signals demonstrate broader global significance, reflecting their extensive involvement in regulation and coordination of different physiological processes, including functional integration similar to that observed in default mode network dynamics [43]. Additionally, under LALV, while the G-Strength of node D1 in HRV system declines, its B-Strength increases, underscoring the necessity of examining constituent physiological activities within a single system at a finer level of detail. This approach reveals the rich diversity of roles these activities play. (2). Betweenness serves as a critical metric to elucidate the work

efficiency of each node or physiological activity within the network, underscoring its intermediary role in information transmission and system integration. In HAHV, the integration and processing of emotional responses heavily depend on EMG and RSP patterns, highlighting their essential functions. Conversely, in HALV and LAHV, GSR system predominantly facilitates multi-system integration. Narrowing the research focus further reveals a rich diversity in work efficiency among physiological activities. Specifically, in HALV, the two types of Betweenness centrality of the E10 node apparently increases, representing sample entropy in the EEG gamma band, indicating its heightened efficiency in information transmission across brain regions or physiological systems. In contrast, within the GSR system in HALV, nodes G5 and G6 primarily function as cross-system intermediaries which excel at information exchange between GSR system and other physiological systems. However, nodes G7 and G8 within GSR system do not demonstrate enhanced processing efficiency but rather exhibit relatively independent operation in HALV. (3). ExpectedInfluence quantifies the combination of synergistic and inhibitory effects. At the system level, the B-ExpectedInfluence of EEG signals not only exhibit polarity changes, but also quantifies the intensity of central regulation. For instance, the absolute value of negative G-ExpectedInfluence in high-arousal emotions is strongly greater than the positive G-ExpectedInfluence value in LALV, reflecting the intensity difference between strong central inhibition of irrelevant signals and weak cooperation during low arousal. At the node level, the positive intra-system G-ExpectedInfluence values of nodes E1-E6 in EEG signals are strongly higher than their negative cross-system values, reflecting the ratio of cooperation among brain regions to the intensity of peripheral filtering. The negative cross-system G-ExpectedInfluence value of HRV increases with heightened emotional arousal, reflecting changes in the intensity of parasympathetic nervous system inhibition on peripheral variation, which is consistent with meta-analytic findings linking HRV to neurophysiological markers of stress [44]. At the node level, the distinction for D1 in HRV system between negative intra-system G-ExpectedInfluence and positive cross-system G-ExpectedInfluence encapsulates the comparison between parasympathetic and sympathetic regulation of the heart rate.

D. Limitations and Future Directions

This study has the following limitations, which could be addressed in future work: (1). Building on research linking resting-state connectivity abnormalities to major depressive disorder and efforts to define circuit-based biotypes for mood disorders [40], [45]. future work should leverage network analysis to identify disease-specific biomarkers by longitudinally comparing PANs in pathological versus healthy states. (2). One limitation of the current model is its reliance on undirected graphs, which capture statistical associations but not causality. Future studies with directed networks and directional weights could quantify causal influences, enhancing analytical depth, and refining understanding of physiological interactions. Additionally, non-invasive brain stimulation could be employed to validate the causal relationships inferred from these networks [46], paving the way for targeted therapeutic modulation of physiological interactions. (3).This study does not involve individual-level network research, and future studies can further refine the analysis of individual-level PANs.

V. Conclusion

In summary, our study proposes a novel PAN framework to address the limitation of traditional physiological network analysis that neglects heterogeneous intra-system activities. By extracting emotion-sensitive physiological attributes from six types of signals, the framework enables fine-grained analysis of intra- and inter-system interactions. Key findings reveal that physiological activities exhibit diverse and state-dependent roles, dynamic synergistic/inhibitory interactions, and adaptive network topology variations across four emotional states. Network comparison and centrality analyses validate the framework's robustness and uncover system-specific interaction patterns. This work pioneers topological characterization of physiological attributes, offering a new perspective for physiology and disease research. It holds promise for clinical applications in diagnosis and health management, while future directions include extending to clinical populations, integrating multi-modal data, and developing directed network models to explore causal relationships.

References

[1] T. Engelen, M. Solcà, and C. Tallon-Baudry, "Interoceptive rhythms in the brain," *Nat Neurosci*, vol. 26, no. 10, pp. 1670–1684, Oct. 2023.

[2] M. Sammons, M. C. Popescu, J. Chi, S. D. Liberles, N. Gogolla, and A. Rolls, "Brain-body physiology: Local, reflex, and central communication," *Cell*, vol. 187, no. 21, pp. 5877–5890, Oct. 2024.

[3] Y. Liu et al., "Cognitive Load Prediction From Multimodal Physiological Signals Using Multiview Learning," *IEEE Journal of Biomedical and Health Informatics*, vol. 29, no. 5, pp. 3282–3292, 2025.

[4] T. Oyelade, K. P. Moore, and A. R. Mani, "Application of physiological network mapping in the prediction of survival in critically ill patients with acute liver failure," *Sci Rep*, vol. 14, no. 1, p. 23571, Oct. 2024.

[5] R. P. Bartsch, K. K. L. Liu, A. Bashan, and P. C. Ivanov, "Network Physiology: How Organ Systems Dynamically Interact," *PLoS One*, vol. 10, no. 11, p. e0142143, 2015.

[6] A. Bashan, R. P. Bartsch, J. W. Kantelhardt, S. Havlin, and P. C. Ivanov, "Network physiology reveals relations between network topology and physiological function," *Nat Commun*, vol. 3, no. 1, p. 702, Feb. 2012.

[7] M. Massimini, F. Ferrarelli, R. Huber, S. K. Esser, H. Singh, and G. Tononi, "Breakdown of Cortical Effective Connectivity During Sleep," *Science*, vol. 309, no. 5744, pp. 2228–2232, Sept. 2005.

[8] T. W. Boonstra, A. Danna-Dos-Santos, H.-B. Xie, M. Roerdink, J. F. Stins, and M. Breakspear, "Muscle networks: Connectivity analysis of EMG activity during postural control," *Sci Rep*, vol. 5, p. 17830, Dec. 2015.

[9] Z. Cai, H. Gao, M. Wu, J. Li, and C. Liu, "Physiologic Network-Based Brain-Heart Interaction Quantification During Visual Emotional Elicitation," *IEEE Trans Neural Syst Rehabil Eng*, vol. 32, pp. 2482–2491, 2024.

[10] P. C. Ivanov, "The New Field of Network Physiology: Building the Human Physiolome," *Front Netw Physiol*, vol. 1, p. 711778, 2021.

[11] D. Candia-Rivera, V. Catrambone, J. F. Thayer, C. Gentili, and G. Valenza, "Cardiac sympathetic-vagal activity initiates a functional brain-body response to emotional arousal," *Proc Natl Acad Sci U S A*, vol. 119, no. 21, p. e2119599119, May 2022.

[12] H. A. Shehu, M. Oxner, W. N. Browne, and H. Eisenbarth, "Prediction of moment-by-moment heart rate and skin conductance changes in the context of varying emotional arousal," *Psychophysiology*, vol. 60, no. 9, p. e14303, Sept. 2023.

[13] T. Beatton, H. F. Chan, U. Dulleck, A. Ristl, M. Schaffner, and B. Torgler, "Positive affect and heart rate variability: a dynamic analysis," *Sci Rep*, vol. 14, no. 1, p. 7004, Mar. 2024.

[14] R.-N. Duan, J.-Y. Zhu, and B.-L. Lu, "Differential entropy feature for EEG-based emotion classification," in *2013 6th International IEEE/EMBS Conference on Neural Engineering (NER)*, Nov. 2013, pp. 81–84.

[15] C. L. Brown, N. Van Doren, B. Q. Ford, I. B. Mauss, J. W. Sze, and R. W. Levenson, "Coherence between subjective experience and physiology in emotion: Individual differences and implications for well-being," *Emotion*, vol. 20, no. 5, pp. 818–829, Aug. 2020.

[16] Z. Wang and Y. Wang, "Emotion recognition based on multimodal physiological electrical signals," *Front Neurosci*, vol. 19, p. 1512799, 2025.

[17] R. Jenke, A. Peer, and M. Buss, "Feature Extraction and Selection for Emotion Recognition from EEG," *IEEE Transactions on Affective Computing*, vol. 5, no. 3, pp. 327–339, 2014.

[18] S. Koelstra et al., "DEAP: A Database for Emotion Analysis;Using Physiological Signals," *IEEE Transactions on Affective Computing*, vol. 3, no. 1, pp. 18–31, 2012.

[19] B. E. Ajtay, S. Béres, and L. Hejjel, "The oscillating pulse arrival time as a physiological explanation regarding the difference between ECG- and Photoplethysmogram-derived heart rate variability parameters," *Biomedical Signal Processing and Control*, vol. 79, p. 104033, 2023.

[20] J. Xu, Y. Zhang, M. Xie, W. Wang, and D. Zhu, "Real-time intelligent on-device monitoring of heart rate variability with PPG sensors," *Journal of Systems Architecture*, vol. 154, p. 103240, 2024.

[21] R. Foygel and M. Drton, "Extended Bayesian Information Criteria for Gaussian Graphical Models," Nov. 30, 2010, *arXiv*: arXiv:1011.6640.

[22] J. Friedman, T. Hastie, and R. Tibshirani, "Sparse inverse covariance estimation with the graphical lasso," *Biostatistics*, vol. 9, no. 3, pp. 432–441, July 2008.

[23] D. J. Robinaugh, R. H. A. Hoekstra, E. R. Toner, and D. Borsboom, "The network approach to psychopathology: a review of the literature 2008-2018 and an agenda for future research," *Psychol Med*, vol. 50, no. 3, pp. 353–366, Feb. 2020.

[24] M. Heilbron, K. Armeni, J.-M. Schoffelen, P. Hagoort, and F. P. de Lange, "A hierarchy of linguistic predictions during natural language comprehension," *Proceedings of the National Academy of Sciences*, vol. 119, no. 32, p. e2201968119, 2022.

[25] D. Borsboom and A. O. J. Cramer, "Network analysis: an integrative approach to the structure of psychopathology," *Annu Rev Clin Psychol*, vol. 9, pp. 91–121, 2013.

[26] A. A. Almet, Y.-C. Tsai, M. Watanabe, and Q. Nie, "Inferring pattern-driving intercellular flows from single-cell and spatial transcriptomics," *Nat Methods*, vol. 21, no. 10, pp. 1806–1817, Oct. 2024.

[27] S.-W. Lin and W.-M. Lu, "A comparison of chance-constrained data envelopment analysis, stochastic nonparametric envelopment of data and bootstrap method: A case study of cultural regeneration performance of cities," *European Journal of Operational Research*, vol. 316, no. 3, pp. 1179–1191, 2024.

[28] P. J. Jones, R. Ma, and R. J. McNally, "Bridge Centrality: A Network Approach to Understanding Comorbidity," *Multivariate Behav Res*, vol. 56, no. 2, pp. 353–367, 2021.

[29] M. Rubinov and O. Sporns, "Complex network measures of brain connectivity: uses and interpretations," *Neuroimage*, vol. 52, no. 3, pp. 1059–1069, Sept. 2010.

[30] X.-N. Zuo et al., "Network centrality in the human functional connectome," *Cereb Cortex*, vol. 22, no. 8, pp. 1862–1875, Aug. 2012.

[31] U. Braun et al., "Test-retest reliability of resting-state connectivity network characteristics using fMRI and graph theoretical measures," *Neuroimage*, vol. 59, no. 2, pp. 1404–1412, Jan. 2012.

[32] J. K. Hsieh et al., "Cortical sites critical to language function act as connectors between language subnetworks," *Nat Commun*, vol. 15, no. 1, p. 7897, Sept. 2024.

[33] H. Hintiryan et al., "Neural networks of the mouse visceromotor cortex," *Nature*, Aug. 2025.

[34] I. Stitt, Z. C. Zhou, S. Radtke-Schuller, and F. Fröhlich, "Arousal dependent modulation of thalamo-cortical functional interaction," *Nat Commun*, vol. 9, no. 1, p. 2455, June 2018.

[35] R. Adolphs, "How should neuroscience study emotions? by distinguishing emotion states, concepts, and experiences," *Soc Cogn Affect Neurosci*, vol. 12, no. 1, pp. 24–31, Jan. 2017.

[36] M. Picó-Pérez et al., "Dispositional use of emotion regulation strategies and resting-state cortico-limbic functional connectivity," *Brain Imaging Behav*, vol. 12, no. 4, pp. 1022–1031, Aug. 2018.

[37] M. Nezafati, H. Temmar, and S. D. Keilholz, "Functional MRI Signal Complexity Analysis Using Sample Entropy," *Front Neurosci*, vol. 14, p. 700, 2020.

[38] M. Amalric and J. F. Cantlon, "Entropy, complexity, and maturity in children's neural responses to naturalistic video lessons," *Cortex*, vol. 163, pp. 14–25, June 2023.

[39] F. Shaffer and J. P. Ginsberg, "An Overview of Heart Rate Variability Metrics and Norms," *Front Public Health*, vol. 5, p. 258, Sept. 2017.

[40] P. C. Mulders, P. F. van Eijndhoven, A. H. Schene, C. F. Beckmann, and I. Tendolkar, "Resting-state functional connectivity in major depressive disorder: A review," *Neurosci Biobehav Rev*, vol. 56, pp. 330–344, Sept. 2015.

[41] K. Friston, "The free-energy principle: a unified brain theory?," *Nat Rev Neurosci*, vol. 11, no. 2, pp. 127–138, Feb. 2010.

[42] K. Nakamura, Y. Nakamura, and N. Kataoka, "A hypothalamomedullary network for physiological responses to environmental stresses," *Nat Rev Neurosci*, vol. 23, no. 1, pp. 35–52, Jan. 2022.

[43] C. S. Hu, Y. Zheng, G. Dong, H. Glassman, C. Huang, and R. Xuan, "Resting state default mode network is associated with wise advising," *Sci Rep*, vol. 13, no. 1, p. 14239, Aug. 2023.

[44] J. F. Thayer, F. Ahs, M. Fredrikson, J. J. Sollers, and T. D. Wager, "A meta-analysis of heart rate variability and neuroimaging studies: implications for heart rate variability as a marker of stress and health," *Neurosci Biobehav Rev*, vol. 36, no. 2, pp. 747–756, Feb. 2012.

[45] L. M. Williams, "Defining biotypes for depression and anxiety based on large-scale circuit dysfunction: a theoretical review of the evidence and future directions for clinical translation," *Depress Anxiety*, vol. 34, no. 1, pp. 9–24, Jan. 2017.

[46] R. Polanía, M. A. Nitsche, and C. C. Ruff, "Studying and modifying brain function with non-invasive brain stimulation," *Nat Neurosci*, vol. 21, no. 2, pp. 174–187, Feb. 2018.